ELSEVIER

Brain Research 958 (2002) 472–487

BRAIN RESEARCH INTERACTIVE

www.bres-interactive.com

Interactive report

Video-oculography in the gerbil

Galen D. Kaufman*

Medical Research Building 7.102, University of Texas Medical Branch, 301 University Blvd., Galveston, TX 77555-1063, USA

Accepted 29 August 2002

Abstract

Normative vestibulo-ocular and optokinetic reflexes (VOR and OKR) and pupil diameter were measured in young adult gerbils using infrared video-oculography with 60 Hz sampling during head-fixed binocular recordings. The pupillary light-sink technique was preferred over a single-beam retinal reflection method because its measurements were less affected by pupil size. Eye movements were generally conjugate with occasional independent saccadic movements, and independent drifting movements in the dark. The horizontal optokinetic response to sinusoidal motion of a randomly spaced white dot pattern was maximal at low velocities (5°/s), stronger temporonasally, and dropped off quickly at ~20°/s. Constant velocity gain was near unity through 60–80°/s with a sharp drop-off. Monocular viewing revealed almost no nasotemporal optokinetic response. Pupil diameter was found to vary as a saddle function with optokinetic gain from cycle to cycle, but also have a circadian rhythm (smaller at dusk) that related inversely to mean horizontal VOR gain. Gerbils with eyes open sometimes had no optokinetic response during long stimulus periods, which then resumed after a brief vestibular stimulus. The horizontal angular VOR gain was relatively flat across 0.1–1.0 Hz and 30–120 d/s sines (phase near zero), with a mean gain of ~0.78 in the dark, and 1.0 with the fixed pattern surround ($n=15$, for both raw calibrated and normalized data). Most animals also revealed a strong slow phase eye velocity asymmetry (dominant during ipsilateral rotation) in the half-cycle gain of their horizontal angular VOR response in the dark. A constant velocity horizontal optokinetic bias velocity did not change the gain or symmetry of the sinusoidal VOR response, but shifted the VOR response velocity in an additive (linear) fashion. Both cross-coupling (pitch or roll while rotating) and pseudo-OVAR (off-axis counter-rotation) stimuli generated horizontal nystagmus. The findings suggest that the gerbil, like other lateral-eyed rodents, relies on otolith cues to interpret angular motion.

Theme: Motor systems and sensorimotor integration

Topic: Oculomotor systems

Keywords: Meriones; Rodent; Eye movement; Oculomotor; Coil; Vestibular; Optokinetic; Linear; Centripetal; OVAR

1. Introduction

Video techniques are beginning to gain favor in physiology and genetics laboratories as a simpler method to record the eye behavior of rodents [28,39,40]. We have developed a binocular infrared (IR) video system to record two-dimensional eye movements in the gerbil during experiments that drive plasticity in vestibulo-ocular pathways. Rodent video-oculography improves on the magnetic search coil method by avoiding artifacts (e.g. impeded visual field, topical irritation, or mechanical obstruction) created using scleral-implanted or corneal-attached induction coils [22,33,40]. In our experience, nearly any physical manipulation of the eye can have motor consequences. The drawbacks of video-oculography include unwanted IR reflections, eyelid artifacts, and lower frequency data sampling. Newer camera systems are improving temporal resolution significantly (e.g. SMI at 250 Hz), and can be as accurate as coil systems in most respects [44], and result in higher reported gains compared to coils in rodents [40].

The purpose of this report is to document our method of video-oculography in the rodent, to inform of possible caveats, and to provide normal, binocular oculomotor data from the gerbil species. Many previous studies have investigated vestibular-related neuronal and unit responses in the gerbil, but normative oculomotor behavior was still

*Tel.: +1-409-772-2723; fax: +1-409-772-5893.
E-mail address: gdkaufma@utmb.edu (G.D. Kaufman).

0006-8993/02/$ – see front matter
PII: S0006-8993(02)03557-6

lacking. Our subsequent observations have revealed rodent oculomotor behavior not yet described in the literature, due in part to binocular recordings.

Our choice to use the gerbil as a model for vestibular adaptation includes general factors like ease of breeding, low cost, and the large, delicate middle ear anatomy that makes surgical manipulation of the labyrinth simple. For oculomotor reasons, a rodent model avoids the complication of higher (supracortical) control layers present in primates, so that one can focus on the phylogenetically older vestibular and optokinetic systems [13,31]. In rats, destruction of visual cortex does not seem to affect the optokinetic response [14]. Rodents are generally thought to be afoveate, e.g. Ref. [25], and therefore incapable of training based on target acquisition. However, the mouse has many more rods, and a cone density similar to that of primates outside the fovea [20]. Natural gerbil behavior includes rapid head movements and therefore requires robust vestibulo-ocular and vestibulo-collic responses. Rodents, e.g. rat, clearly utilize otolith information to support their VOR [3], and such studies suggest high sensitivity to otolith input. The presence of a velocity storage mechanism [35] for extending peripheral stimuli in rodents has been controversial. There is definite optokinetic storage [15], but the vestibular response is typically near the relatively short semicircular canal constant of 2.3–4 s in the rat [8].

Our basic examination of the gerbil vestibulo-ocular and optokinetic reflexes (VOR, OKR) supports most of these previous observations, and raises new questions. We describe new findings that have a significant impact on eye movement. These include half-cycle vestibular asymmetries in response to horizontal sinusoidal head motion in the dark, a relationship between pupil diameter and optokinetic gain, and an optokinetic constant velocity bias response that shifts VOR velocity linearly, but does not change the overall gain. In addition, we present preliminary data showing circadian effects on the vestibular system, and evidence that, as in other animals, the gerbil utilizes otolith information to help calculate angular velocity during constant motion.

2. Methods

Thirty-eight gerbils (*Meriones unguiculatus*) of both sexes between 60 and 80 g were used to develop these techniques, or are represented in the data. All procedures conform to the *Guide for the Care and Use of Laboratory Animals* (NIH Publication No. 86-23, revised 1996).

For measurement of the OKR and VOR, we developed an alert gerbil preparation in which a head restraint bolt was surgically implanted at least 3 days prior to the recording session. The position of the gerbil's head in the stereotaxic device had the nose bar 8 mm down from ear bar horizontal, resulting in an earth horizontal plane for the horizontal canals [30]. Initially the bolt was held in place by dental cement hardened by cyanoacrylate over screws placed into the skull. Self-tapping stainless steel screws (≠00, 0.125 inches, www.smallparts.com) were placed at eight points as anchors for the acrylic cap, which fixed the hardware together. In some cases small lesions were observed corresponding to the tip of the implant screws in the underlying cortex after this method. Some implants also failed to hold and were torn out with vigorous activity, usually after 1 week or more. Therefore, this technique has since been refined to avoid the use of skull screws altogether. By cleaning and scoring the skull surface and applying a hydrophilic cyanoacrylate adhesive (e.g. Loctite 4541, Prism Medical Device), followed by dental acrylic, a strong bond forms between the glue and the skull, and no penetration into the dura by skull screws was necessary. The animals were restrained for several hours during testing without implant failure, and re-tested for several weeks if necessary. The footprint of the dental acrylic on the skull covers the dorsal surface (up to the parietal ridge) but should not extend too far laterally, or cause a ridge of skin to form above the eyes, which can cause ptosis and therefore poor data. It was more difficult to acquire a good eye image in older animals (above 80 g), primarily from a tendency for the upper eyelid to droop. Following the surgery and for the extent of its use, each animal was housed individually to protect the implant. The colony and implant animals were maintained in the lab where windows provided natural lighting conditions.

Two dimensional eye movements were recorded using ISCAN (RK-426) equipment. Two 50 mm (1:1.8, V5018, Edmund Science) lenses and cameras (model 20A698, C/CS, genlockable, EIA monochrome, 1/3 inch CCD, from Videology Imaging Solutions) were placed lateral to the animal on a turntable (Fig. 1). Each eye signal was in sync with a small wide-angle camera, providing the operator with a view of the gerbil and stimulus motion (3.7 mm, PC72, SuperCircuits). The iral image was reflected on an IR dichroic mirror to preserve the animal's field of view. Two methods were tested to isolate pupillary movement: (1) retinal reflection (the 'red-eye' phenomenon), and (2) pupil light sink (e.g. Fig. 1B). We explored the first method because of concerns that the gerbil iris would not provide enough contrast from the dark pupil for proper thresholding. For illumination in the dark a single IR diode was placed directly in front of the camera lens on the optic axis of the measured eye, and its reflection off the retina back through the lens and cornea was tracked by the ISCAN corneal reflection circuit as a light centroid. A slight modification to the circuitry allowed the light, rather than dark, pupil centroid diameter to also be recorded in this configuration, providing the additional data about the autonomic balance of the animal. Because the pupillary diameter varies often, which then affects the amount of light reflecting back from the retina, using the retinal reflection technique required constant adjustment of the

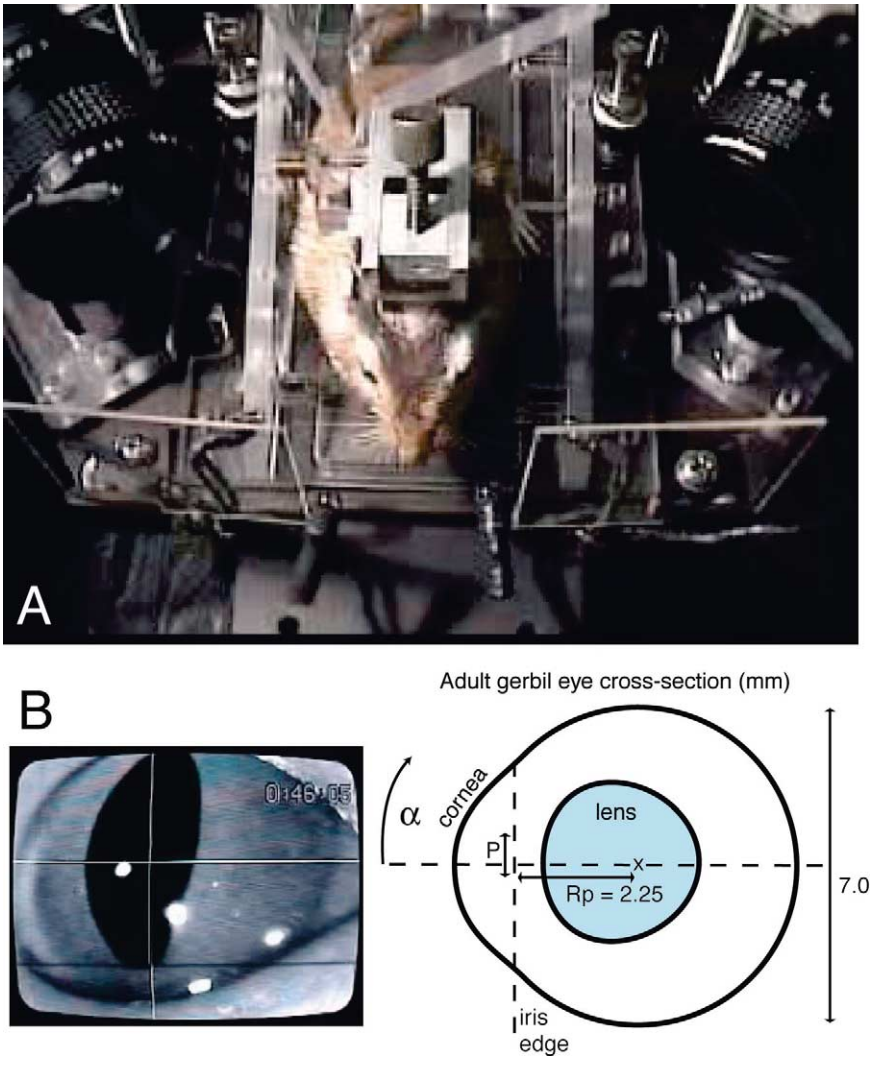

Fig. 1. (A) A head-restrained gerbil in the centrifuge restraint. Three infrared diodes, a camera, and dichroic mirror are positioned to record each eye, while preserving most of the animal's field of view. (B) A video frame from an eye during recording. The vertical and horizontal white lines correspond to the ISCAN output fitting the dark pupil center (threshold not shown). The white dots are reflections of the illuminating infrared diodes. Also shown is a cross-sectional profile of the adult gerbil eye, and the mean distances used to calibrate the eye video signal. The gerbil lens is large compared to the overall globe: a distance of 2.25 mm from the center of eye rotation to the edge of the iris defines the geometric relationship of actual rotation in degrees to what the camera 'sees' as translation of the pupil centroid. See Section 2 for detail.

ISCAN threshold to collect a good eye signal. In these animals, topical epinephrine (one drop of 1% solution) ensured mydriasis for a robust pupil signal, eliminating the need for constant threshold adjustment but preventing information about the autonomic system. A wide pupil, however, also creates measurement artifacts by at least two mechanisms: losing the pupil edge under an eyelid or canthus, and spherical distortion during lateral movement.

Therefore, we switched back to the standard procedure of flooding the eyes with IR light directly from several oblique angles, and detecting the dark pupil as a light sink, using the factory standard ISCAN circuitry. The threshold during the light sink technique was less sensitive to pupillary diameter changes without applying epinephrine. Therefore, the dark pupil method required less monitoring and was more robust. However, if autonomic data was not desired, the topical application of pilocarpine (resulting in miosis; a muscarinic cholinergic agonist and therefore unlikely to affect oculomotor function) produced optimum results in the light-sink method. A small pupil aperture was less likely to disappear behind the eyelid and cause measurement artifacts.

We used IR diodes (three for each eye, with 8 or 20° beams) with a peak emission wavelength of ~920 nm—slightly farther from the visual spectrum than typical IR diodes—in order to avoid any possible sensitivity. Gerbil retina is ~87% rods and is known to possess unusual wavelength sensitivity, at least blue-green [12] and perhaps ultraviolet [18]. Although the range of pixel values between the pupil and surrounding corners of the eye was

often narrow, adjusting the IR diode positions and closing the camera f-stop aperture was often sufficient to collect a good pupil signal.

It was important to prepare the eyes for the best image possible. In order to do so, as we developed the technique, early animals were anesthetized briefly using isoflurane inhalant gas (3% induction, 1.5% maintenance) just prior to recording. These procedures included some, but not all, of the following, depending on the method applied:

1. Trimming the eyelashes and vibrissae, which can interfere with the camera path to the pupil
2. Marking the eyelids black to decrease unwanted reflection during the retinal reflection technique
3. Applying topical drugs to the cornea:
   (a) epinephrine (1% for mydriasis, autonomic data lost)
   (b) pilocarpine (1% for miosis, autonomic data lost)
   (c) lidocaine (2% gel for topical anesthesia)
4. Placing upper eyelid sutures (to hold the eye open during recording for vertical signals, in combination with lidocaine anesthesia)

These procedures generally took less than 5 min. Eventually we began trimming the vibrissae and eyelashes during the implant procedure, so that on the day of testing the animal could be restrained without anesthesia or further eye preparation. Monocular recording was accomplished by carefully (under isoflurane anesthesia) gluing the eyelids of one eye closed with a cyanoacrylate-based adhesive, while allowing the globe underneath to move freely.

Eye movement was calibrated by first fitting a linear voltage relationship using a moving spot against a measured millimeter grid in the camera field. The degree of eye rotation was then calculated on-line during data acquisition in LabView using the geometrical relationship of eye radius to the two-dimensional translation detected by the camera [40] (Fig. 1B). Although the precise geometry is not linear, for 5–10° movements near the optic axis, it is a reasonable approximation. Briefly:

$$\alpha \text{ (degrees)} = \arcsin(P/Rp)$$

where P = linear pupil centroid displacement and Rp = the rotational radius of the eye (~2.25 mm)

We used animals of similar age and weight for our tests, but individual variations in ocular size and geometry are possible. Therefore, in order to adjust for small differences in image focal length and calibration differences between left and right eye and across animals, the optokinetic and vestibular response gains presented here were normalized for statistical comparisons. Each animal's mean VOR gain (over 20 or more cycles) in the light during horizontal 1.0 Hz, 60°/s maximum velocity sinusoids was used as the 100% gain value for that animal. The gain values for other stimuli were then adjusted by dividing each value for that animal by the 100% gain value. This can distort the true scaling between frequency and amplitude. However, the absolute difference between raw and normalized mean horizontal VOR gain in our dataset ($n = 15$, dark and light) was less than 2%, indicating that our raw data was near absolute values.

Natural vestibular and optokinetic stimulation was provided using a four-axis device designed for our lab (Fig. 2, Bill Crosier, EE; Robert Orton, ME). The four axes include:

1. A 30 lb-ft DC torque motor (Neurokinetics model 495-69) for rotation about an earth vertical axis. A horizontal arm mounted in the center to this motor supports the remaining axes on one end, and control and power equipment for counterbalance on the other end. These two packages are mounted to a center-reversed manual screw drive that can change the effective radius of the animal's position relative to the main rotor
2. A horizontal (eccentric rotary stage) turntable
3. On top of axis 2, where the animal is restrained, a tilt platform that can be positioned for roll or pitch tilt (±30°)
4. Finally, an optokinetic drum surrounding the animal and the eccentric and tilt axes for horizontal visual stimulation (not shown in Fig. 2)

All of the axes are capable of independent or simultaneous control (axes 2–4 use Galil servomotors, model 50-1000, peak torque 1.45 Nm). The eccentric axis control can be slaved to the main axis velocity feedback signal in any ratio (positive or negative); as can the optokinetic axis be slaved to the eccentric axis. Horizontal velocity steps can be generated with an acceleration of ~500°/s/s. Lights and an alerting tone can be activated through the software interface. The optokinetic stimulus consisted of a dimly lit, high-contrast, patterned visual surround (randomly placed white dots of 8.1 and 1.7 visual degrees (3.8 and 0.8 cm) against a black background at a radius of 27 cm, with a mean lux on the wall of 0.026). The animal's field of view was relatively unimpeded (Fig. 1A) and extended over 180° at most elevations. Some initial testing was done using vertical stripes, but this resulted in lower gains and the possibility for vertical retinal slip. No eye response occurred when the light-tight optokinetic drum was moved in the dark (data not shown).

During recording, 16 channels of 60 Hz data, including left and right eye horizontal and vertical position and pupil diameter (and corneal reflection channels), and both velocity and position profiles of the motion control axes, were fed through a National Instruments data acquisition

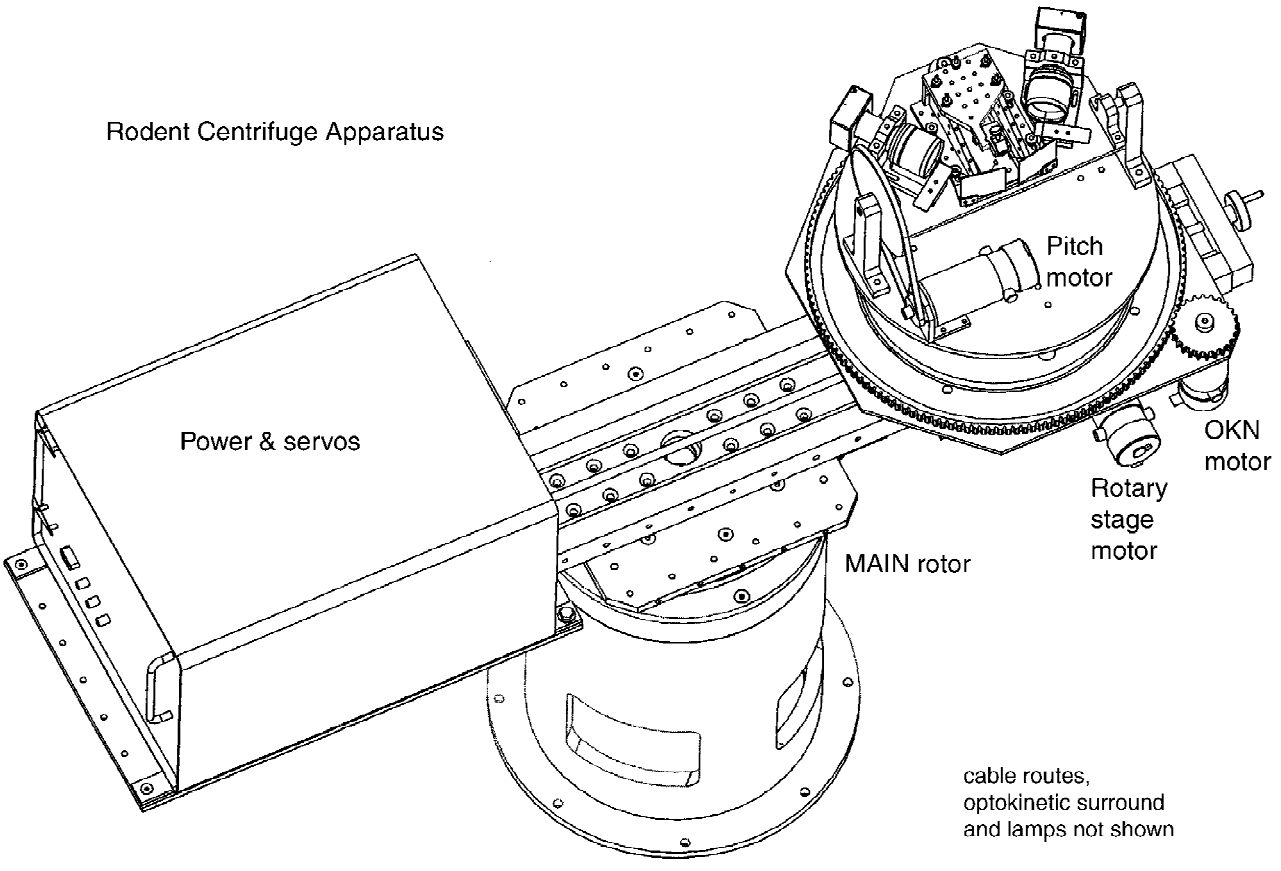

Fig. 2. Centrifuge schematic—the device consists of four independent rotational axes: (1) the main earth-vertical rotor, (2) an eccentric earth-vertical (rotary stage) turntable, (3) a pitch (or roll) platform (±30°) where the animal and cameras are mounted, and (4) a horizontal optokinetic surround (drum not shown). Power and servo equipment counterbalance the load on a center-reversed linear slide.

board (16E-4). Eye position data was de-saccaded based on an acceleration or jerk filter off-line, and fit to the sinusoidal stimulus to calculate gain and phase. Whole-cycle stimulus–response analysis was performed using a 5th-order (statistically determined) polynomial fitting algorithm in LabView (Randy Riggs, Applied Innovation, Houston, TX), adopted from previous monkey work [C.M. Stewart et al., personal communication]. This method was used as an alternative to sine fitting because of the intermittent nature of the data (de-saccaded), and the observed asymmetries in the response (see Section 3; a sine would force an average between min and max). The algorithm also uses short samples of bordering data from adjacent cycles to improve the fit. Automated processing capable of global cut-off filters was used, but each fitted cycle was examined and discarded if necessary. Half-cycle fits were performed using linear regression of the binned leftward or rightward slow-phase cycle points in a sample. Phase fits on the eye data were corrected for the 16.6 ms sample delay generated from the ISCAN system (6° at 1.0 Hz). For some statistical and graphing analysis, binary and text data was exported to other programs (Excel, IGOR). Because of the low sampling rate, testing above 1 Hertz would not provide enough data points for accurate slow-phase fitting. Since the lab's primary interest involves otolith responses, this restriction is less critical provided that the targeted responses involve low-frequency behavior.

Fig. 3. Pupil diameter correlates with changes in optokinetic and vestibular gain. (A) Fitted right eye horizontal optokinetic gain (dots) and right eye pupil diameter (line) during horizontal optokinetic sinusoidal velocity (±10 d/s, 0.5 Hz, not shown). For each fitted cycle the optokinetic response gain generally increased with pupil diameter, but the relationship is noisy and not necessarily linear (see text). (B) Later, in the same animal as shown in A, the right eye was treated topically with 1% pilocarpine to force miosis. The linkage between pupil diameter and optokinetic response gain appears to remain in both eyes. Also note that gains were higher in both eyes, and the pupil diameter was lower in the untreated eye, during the latter testing period with pilocarpine compared to A. (C) Mean pupil diameter and horizontal angular VOR gain in the dark (0.5 Hz, 60 d/s), respectively, in one animal during a 36-h testing period (±S.E.). Each time point represents the mean of 200 s of sampling, and intermittent data is overlaid (i.e. closely spaced time points represent similar time points 24 h apart). The VOR response gain increased when pupil diameter was low and more variable late in the day. Fitted lines are sinusoidal.

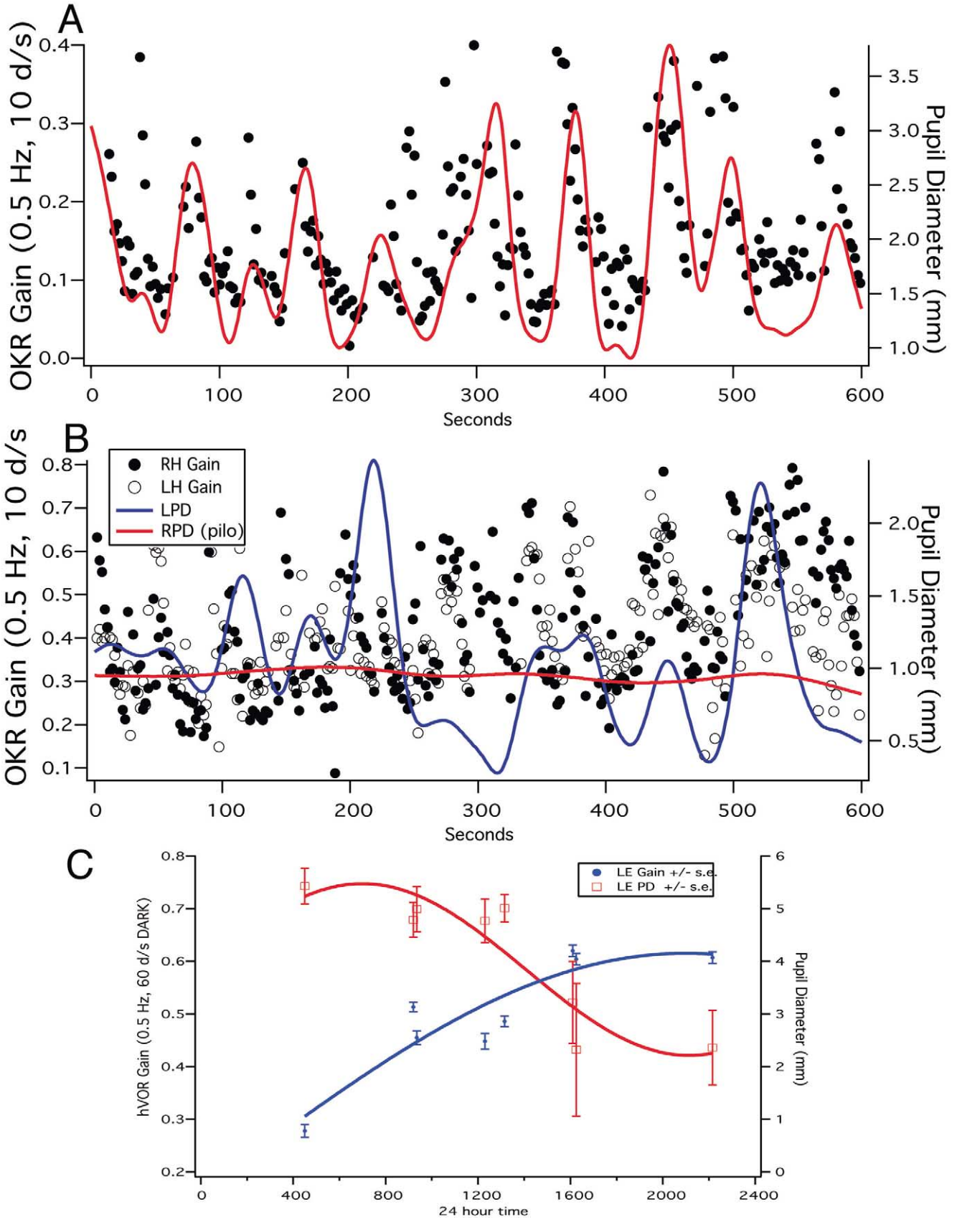
A
OKR Gain (0.5 Hz, 10 d/s)
Pupil Diameter (mm)
Seconds
B
RH Gain
LH Gain
LPD
RPD (pilo)
OKR Gain (0.5 Hz, 10 d/s
Pupil Diameter (mm)
Seconds
C
LE Gain +/- s.e.
LE PD +/- s.e.
hVOR Gain (0.5 Hz, 60 d/s DARK)
Pupil Diameter (mm)
24 hour time

3. Results

3.1. Spontaneous eye movements, pupil diameter, and circadian rhythms

It is clear that the gerbil has some ability to move its eyes independent of a stimulus. We regularly observed brief periods of spontaneous eye movements (saccadic gaze shifts) while the animal was restrained without visual or body motion. These were primarily binocular conjugate and horizontal but occasionally divergent, especially while drifting in the dark.

Pupil diameter (PD) varied widely. During complete miosis (parasympathetic autonomic drive), the pupil appeared as a vertical slit approximately 0.5 mm wide. After full mydriasis (sympathetic drive), the aperture was round and over 5 mm in diameter. Pupil diameter could often be directly correlated to the arousal state of the animal, but at other times seemed to cycle regularly over a period of 2–3 min for extended periods of time with no overt change in other behavior (struggling, etc). On average, pupil diameter was greater in the dark.

Pupil diameter was observed to vary reproducibly with the gain of the sinusoidal optokinetic reflex from cycle to cycle (Fig. 3A). In contrast, during horizontal head rotation in the dark, there was no clear indication that instantaneous PD also correlated with vestibular gain from cycle to cycle. The relationship between pupil diameter and optokinetic gain was not always linear. Although in general an increase in PD accompanied an increase in the fitted OKR gain, raw eye velocity data revealed that extremely narrow pupils were also concurrent with higher gains, creating a saddle function for OKR gain versus PD (not shown). The minimum OKR gains occurred when the pupil was ~1.5 mm in diameter. Regression of our PD to OKR gain data rarely exceeded an r^2 of 0.3, but visual inspection of the raw data supports the relationship. When 1% pilocarpine was applied to one eye topically to force miosis (Fig. 3B), the loose relationship between PD and OKR gain held in both eyes.

Over a longer time frame, we also noticed that eyelid position and pupil diameter during our recording sessions changed depending on the time of day. Mean pupil diameter over a circadian cycle related inversely to horizontal VOR gain in the dark. Specifically, we observed that pupil diameter was narrow and more variable in the afternoon and dusk, and wider near dawn. Repeated testing of the horizontal angular VOR showed that the mean response gain could vary by as much as 0.3 with these changes (Fig. 3C). These findings were similar in three animals.

3.2. Optokinetic stimulation

For horizontal sines, OKR response gains approached one near 5°/s maximum velocity, and dropped quickly beyond 20°/s (Fig. 6E, F). The well-documented temporonasal (TN) horizontal optokinetic dominance of lateral-eyed species was also observed in the gerbil. During moderate sinusoidal velocities, a bracket-shaped waveform could be observed, showing greater sensitivity at the lower velocity portions of the stimulus (Fig. 4A).

Constant velocity visual field motion during sinusoidal angular head rotation produced a velocity shift in the combined OKR/VOR response. That is, isoplanar optokinetic bias velocity has a linear relationship with slow phase eye velocity (SPEV) during horizontal head rotations, but does not change the gain of the response. For example, during a 20°/s optokinetic bias velocity, an animal experiencing a 90°/s maximum velocity horizontal head sinusoid will generate a peak SPEV of ~110°/s during movement opposite to the optokinetic drum, and ~70°/s during movement in the same direction as the drum, while the whole cycle gain remains consistent with that during a fixed surround. This was true for both half-cycle and full cycle analysis. Fig. 4B shows the fitted SPEV response in a similar situation for three tested frequencies (0.2, 0.5, and 1.0 Hz) at 30 d/s maximum angular velocity, and with concurrent ±20 d/s optokinetic bias. Small eye-dependent temporonasal and bias direction phase differences in the responses could be observed (model inset), but the velocity shift was highly linear across a wide range of bias velocities and testing frequencies.

Vestibular input could re-engage optokinetic sensitivity. We observed several gerbils that were capable of ignoring or suppressing the optokinetic surround velocity that otherwise would have elicited a response, even while their

Fig. 4. More optokinetic responses. (A) A bracket waveform (inset) in the eye position response could be observed during intermediate velocity (e.g. ±45 d/s) horizontal optokinetic sines, caused by the greater response gain during lower stimulus velocities. The main graph shows 5th-order polynomial fits to the slow phase eye velocity response for both eyes from the same data. The sinusoidal gain peaks at approximately ±30 d/s. A temporonasal preference in each eye is also evident. (B) Constant optokinetic bias velocity shifts the sinusoidal horizontal VOR response velocity in the light in a linear fashion. Shown are gaussian fits to the slow phase eye velocity data at 0.2, 0.5 and 1.0 Hz during either 20 d/s rightward or 20 d/s leftward constant optokinetic velocity. Inset: a simple model for the optokinetic bias VOR response has each eye deviating slightly from the apparent optokinetic surround velocity (calculated by subtracting the optokinetic bias velocity from the horizontal stimulus velocity). The deviations correspond to temporonasal asymmetries. (C) Horizontal optokinetic response during a constant velocity (50 d/s rightward) stimulus. The top trace (dark line) shows the typical continuous response of the right eye during binocular vision. The bottom trace (lighter line) shows the right eye several minutes later not responding to the visual surround. A brief horizontal head rotation (0.5 Hz, 60 d/s, black line) re-starts the optokinetic response. (D) Example of a rapid optokinetic response cut-off during high velocity horizontal stimulation. A leftward horizontal optokinetic velocity step from 90 to 100 d/s is shown (having increased stepwise from 0), and the response quickly stops. The velocity where this occurred varied widely with animal and direction (leftward or rightward), and was typically asymmetric.

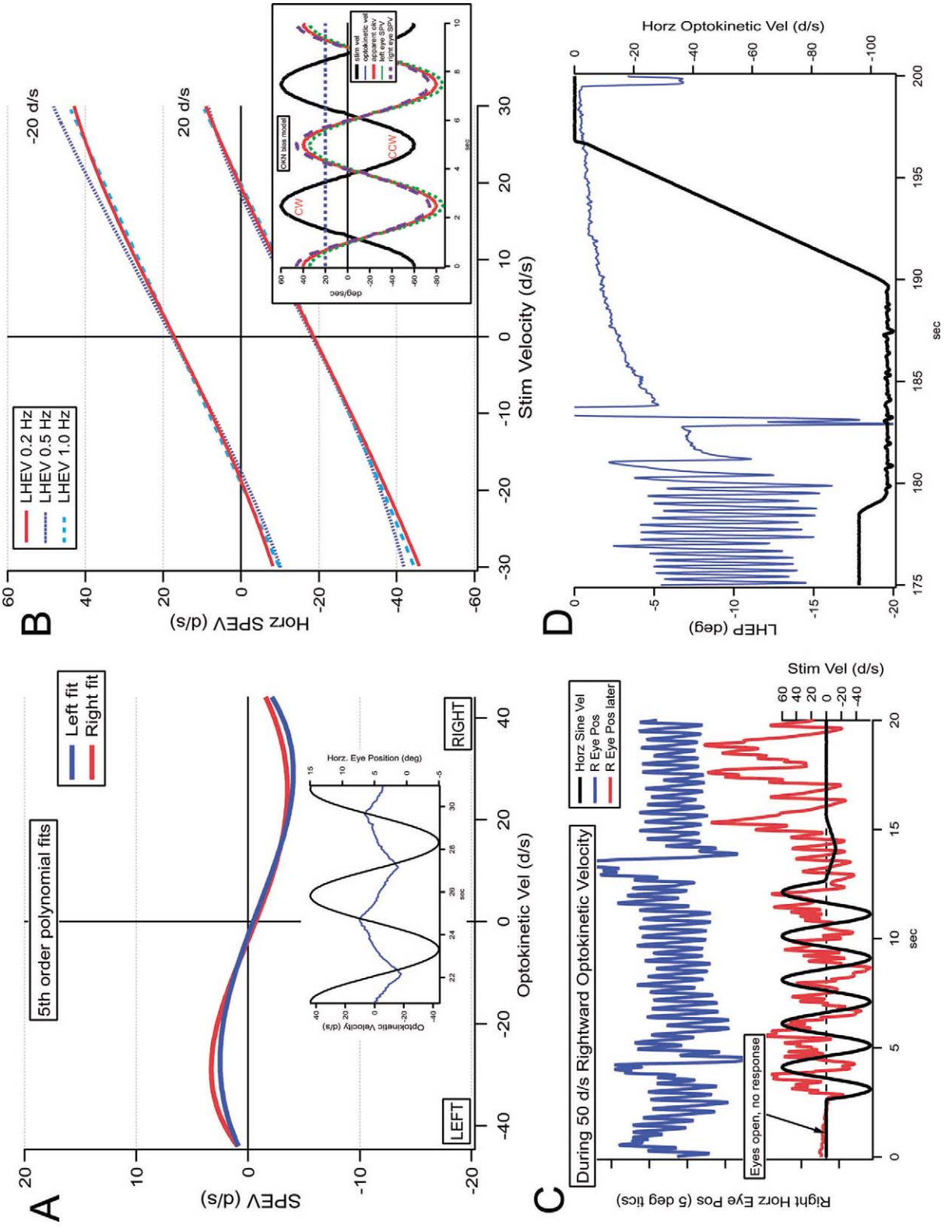
A
SPEV (d/s)
Optokinetic Vel (d/s)
5th order polynomial fits
Left fit
Right fit
LEFT
RIGHT
Horz. Eye Position (deg)
Optokinetic Velocity (d/s)
sec
B
Horz SPEV (d/s)
Stim Velocity (d/s)
-20 d/s
20 d/s
LHEV 0.2 Hz
LHEV 0.5 Hz
LHEV 1.0 Hz
OKN bias model
CW
CCW
deg/sec
stim vel
optokinetic vel
left eye SPV
right eye SPV
C
During 50 d/s Rightward Optokinetic Velocity
Horz Sine Vel
R Eye Pos
R Eye Pos later
Eyes open, no response
Right Horz Eye Pos (5 deg tics)
Stim Vel (d/s)
sec
D
Horz Optokinetic Vel (d/s)
LHEP (deg)
sec

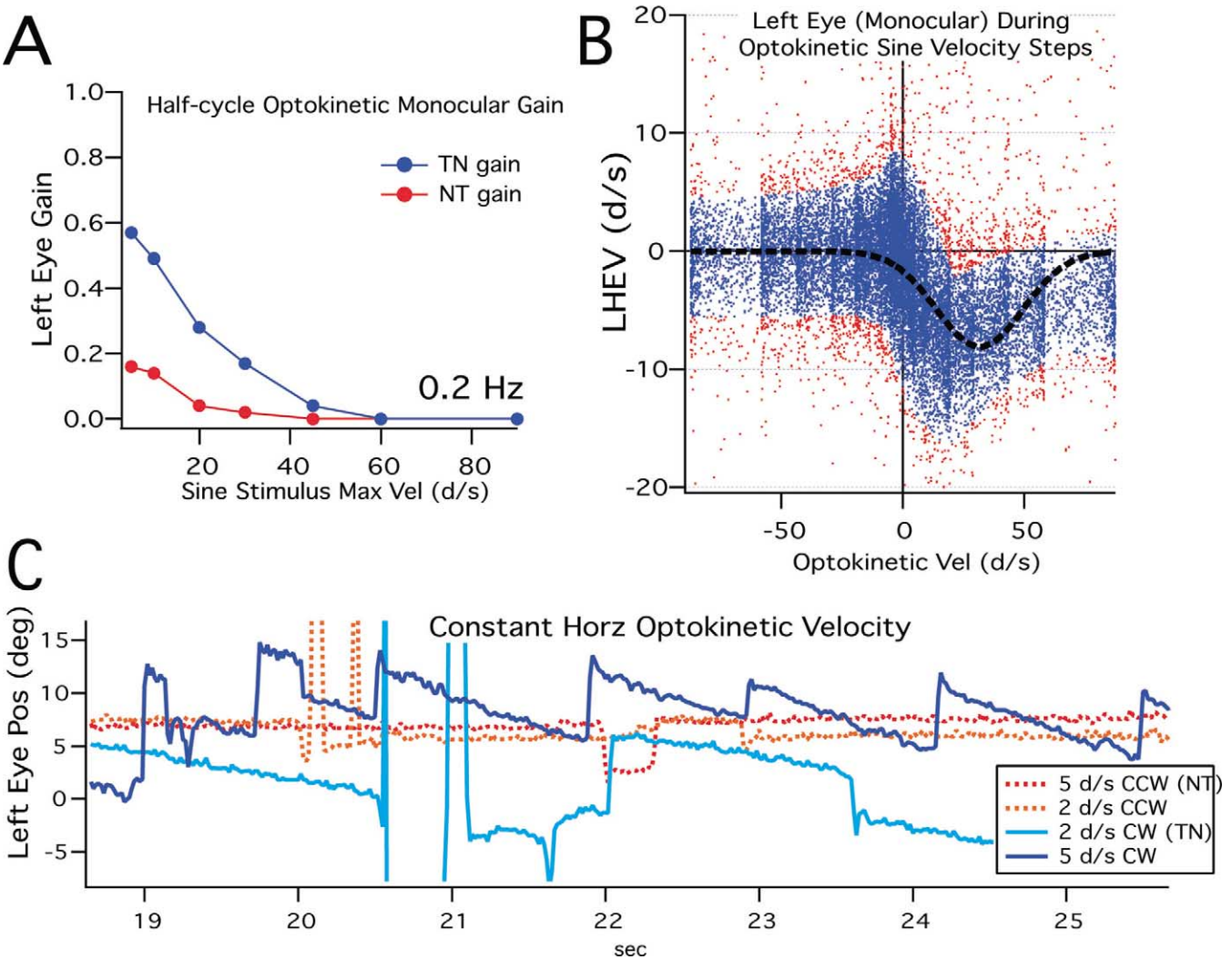

Fig. 5. Monocular optokinetic responses (left eye) in an animal with the right eye closed. (A) Half-cycle fits reveal this monocular optokinetic response gain profile for the left eye during sinusoidal stimulation (0.2 Hz). There is little to no response in the nasotemporal direction. (B) Gaussian fit (dashed line) to slow phase left eye velocity (dark dots) versus horizontal optokinetic stimulus velocity (±100 d/s in 10-d/s steps). Only rightward (temporonasal) motion shows a consistent response, which peaks around 30 d/s. (C) Constant velocity horizontal position traces (left eye, ±2 and 5 d/s) in the temporonasal (TN, solid) and nasotemporal (NT, dashed) directions. Only TN responses are evident.

eyes were clearly open. These periods of no eye movement, lasting up to several minutes, could be ended reliably by applying a brief vestibular motion stimulus, after which the optokinetic response returned (Fig. 4C).

Constant velocity optokinetic stimulation extended sinusoidal sensitivity to approximately 60–80°/s before dropping precipitously. This disengagement of the optokinetic response could happen suddenly, as if a switch were thrown (Fig. 4D). Optokinetic stimulation could also suppress VOR reflexes when conflicting with vestibular input. For example, when a horizontal angular velocity ramp (10 d/s/s) was applied to a head-fixed animal, the typical nystagmus in the dark could be completely suppressed if the animal was surrounded by a subject-stationary visual surround (not shown). Therefore, the OKR can act dominant over the VOR during low threshold, low frequency stimuli.

Monocular horizontal optokinetic stimulation (with the opposite eye closed) elicited a response in the TN direction, but a very limited response in the NT direction.

Fig. 6. Normalized gerbil horizontal VOR and OKR gain responses. (A, B) VOR response gain and phase as a function of maximum sinusoidal stimulus velocity (at 0.5 Hz) in the dark and with the spotted optokinetic surround. (C, D) VOR response gain and phase as a function of stimulus frequency (at 60 d/s maximum velocity) in the dark and with the spotted optokinetic surround. (E, F) Rightward and leftward response gains during horizontal optokinetic sinusoids at 0.2 Hz across stimulus amplitude using half-cycle analysis for the left (dark dotted line) and right (solid line) eye. Temporonasal stimuli elicited a consistently higher response.

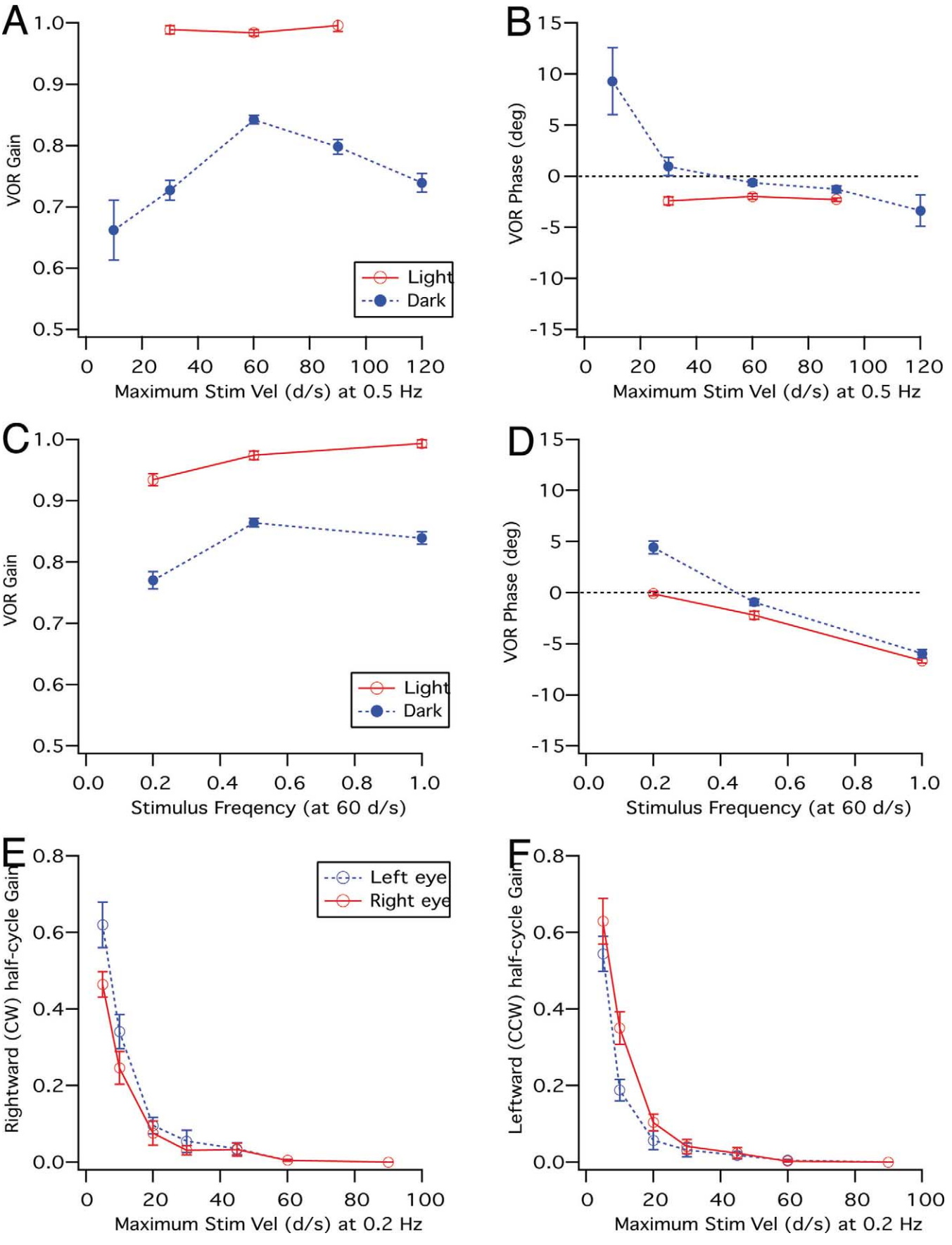
A
VOR Gain
Maximum Stim Vel (d/s) at 0.5 Hz
Light
Dark
B
VOR Phase (deg)
Maximum Stim Vel (d/s) at 0.5 Hz
C
VOR Gain
Stimulus Freqency (at 60 d/s)
Light
Dark
D
VOR Phase (deg)
Stimulus Frequency (at 60 d/s)
E
Rightward (CW) half-cycle Gain
Maximum Stim Vel (d/s) at 0.2 Hz
Left eye
Right eye
F
Leftward (CCW) half-cycle Gain
Maximum Stim Vel (d/s) at 0.2 Hz

Stimulus sinusoids created a horizontal response waveform with only half-cycle sensitivity (Fig. 5).

3.3. Vestibular stimulation

The horizontal angular VOR in our sample ($n = 15$) had a mean gain in the dark (across 0.1–1.0 Hz, and 30–90°/s) of 0.78. With the stationary optokinetic surround illuminated, the mean gain was 1.0 (for both raw and normalized data—defined as 1.0 at 1 Hz, 60°/s). The phase of the eye response was near zero and had a slight phase lag with increasing frequency or amplitude. VOR gain in the dark,

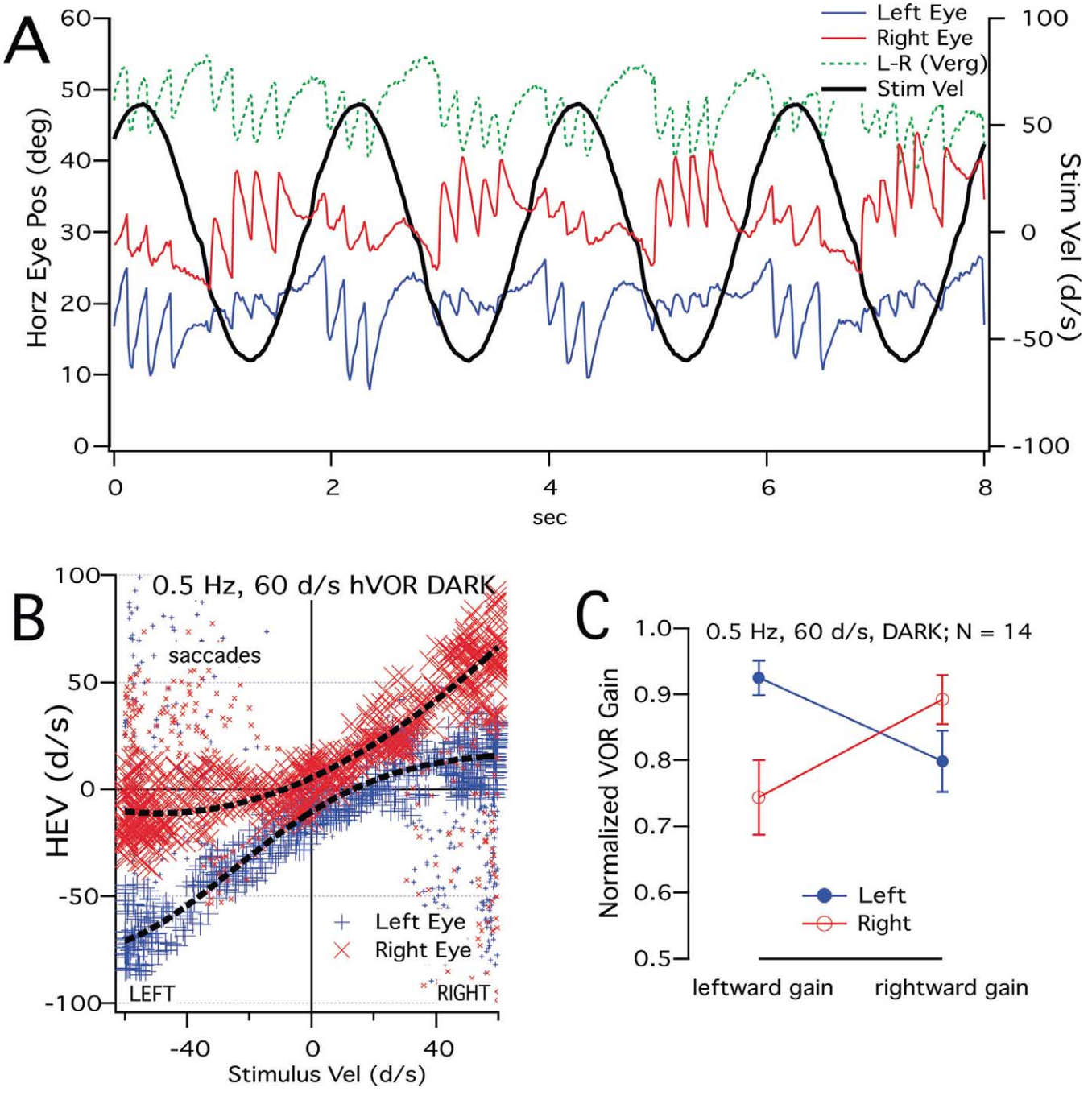

Fig. 7. Vestibular rotational asymmetry. (A) Raw position traces during horizontal rotation in the dark (top dashed trace: difference vergence; middle trace: right eye; bottom dark trace: left eye; thick trace: stimulus—0.5 Hz, 60 d/s maximum velocity—positive is rightward). (B) Slow phase eye velocity from A versus stimulus velocity in the dark. Dotted lines are gaussian fits to the selected slow phase data. Note the ipsilateral turning preference in each eye; a functional match to optokinetic gain asymmetry. (C) Half-cycle analysis of the horizontal angular VOR response gain in the dark in 14 animals at the same stimulus (0.5 Hz, 60 d/s ±S.E.). The response gains vary by ~0.2 depending on rotation direction.

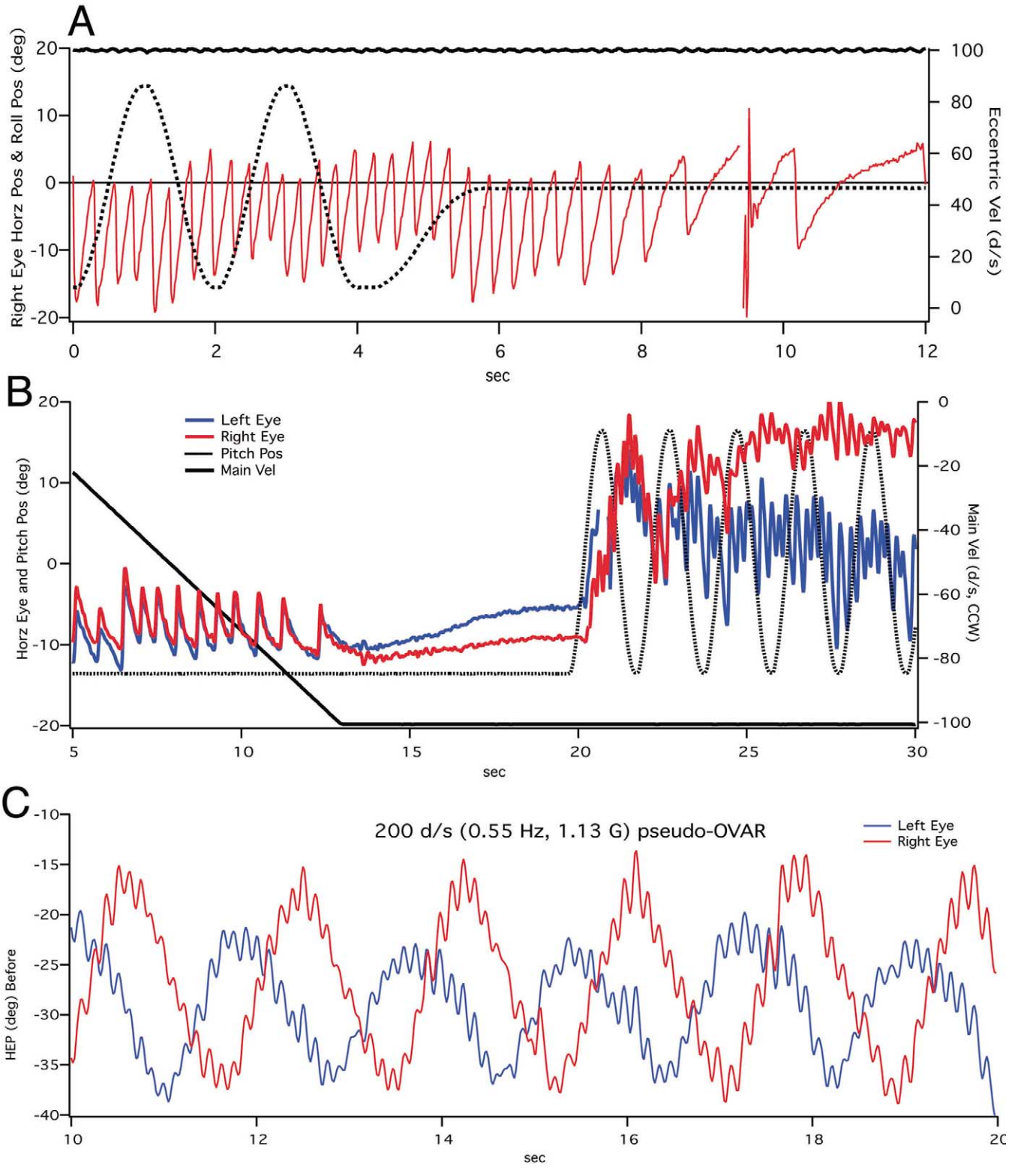

Fig. 8. Continuous horizontal nystagmus is generated during constant velocity rotational motion when combinations of canal and otolith stimuli are applied. Examples shown here include Coriolis (cross-coupling) and eccentric centripetal and counter-rotation stimuli. (A) Right eye position response to a cross-coupling stimulus of 0.5 Hz, ±15° pitch (dotted line) during 100 d/s rightward horizontal rotation (solid line) in the dark. Note the extended response after pitch stop. (B) Cross-coupling plus centripetal stimulus of a 0.5 Hz, ±15° pitch (dotted line) during 100 d/s leftward centripetal rotation (solid line; radius 45 cm, centripetal force of 0.14 G). Horizontal eye position stabilizes as the canal constant is exceeded after the ramp up to constant velocity rotation, then horizontal nystagmus resumes as pitching begins. (C) Eccentric counter-rotation (or pseudo-off-vertical axis rotation) where the main and eccentric horizontal angular velocities are 200 and −200 d/s, respectively (resulting in no relative rotation). The animal's head was 43 cm from the center of main rotation for a resultant (gravity+centripetal) force of 1.13 G, and a rotating vector at 0.55 Hz. Both slow roll motion corresponding to the sweeping resultant vector frequency, and a superimposed linear VOR, can be observed. This is presumably a purely otolith response.

however, peaked at 0.5 Hz and 60°/s, and decreased slightly at higher stimuli (Fig. 6A–D).

We observed asymmetry in the dark in the earth horizontal rotational VOR response similar to that in the optokinetic system. Horizontal rotation that drove the eye in the temporonasal direction (ipsilateral rotation) had a higher gain than nasotemporal slow phases (Fig. 7). This asymmetry was much reduced or absent with a visual surround in the light, varied across individuals in prominence, but was consistently present.

Rotational velocity steps revealed a short vestibular time constant in the gerbil. With accelerations of ~500°/s/s, the vestibular-evoked horizontal rotational nystagmus in the dark lasted only 1–3 s, and showed temporonasal asymmetry. The addition of an optokinetic surround virtually abolished it (not shown).

Vertical eye movements were recorded, but suffered from artifacts due to eyelid occlusion of the pupil, and blinking artifacts. When the animal kept the upper eyelid open and the pupil diameter was small, accurate representations of true vertical movement could be collected. This was especially true using pilocarpine to force miosis. If there was significant ptosis or a wide pupil, the area threshold of the pupil was clipped during vertical movement and resulted in an underestimation of the true vertical (the ISCAN system reports the area centroid). Changes in vertical eye movement behavior must therefore be checked against the overall eye image over time.

The gerbil eye is capable of significant (up to 45°) torsional movements, and although the ISCAN system cannot report torsional movement, playback of the recorded video signal can provide torsional information. Most of the time the gerbil pupil is ellipsoid (Fig. 1B), and the longest chord of the ellipse can be used to determine the angle of rotation over successive frames. Future versions of our software will implement this function. Other investigators have developed software that can track the radial position of iris landmarks using video images.

A preliminary demonstration of the gerbil oculomotor response to coriolis and/or centripetal otolith stimuli is summarized in Fig. 8. Cross-coupling during rotational velocity in two planes helps the gerbil maintain an estimate of a constant primary rotational velocity (Fig. 8A, B). Otolith input alone can generate eye position modulation and linear nystagmus during eccentric counter-rotation (pseudo-OVAR [off-vertical axis rotation], Fig. 8C). Bilateral semicircular canal and otolith inputs combine in the brain to fully represent three-dimensional motion.

4. Discussion

The novel findings in our characterization of normal gerbil oculomotor behavior using video-oculography include:

1. The correlation of pupil diameter with optokinetic gains
2. The ability to suppress optokinetic and vestibular responses
3. A circadian relationship between mean pupil diameter and vestibular gains
4. Significant half-cycle horizontal angular vestibular asymmetries in the dark (ipsilateral turning preference)
5. The sustained induced horizontal nystagmus during both pitch while rotating (PWR) and roll while rotating (RWR, ‘cross-coupling’), and during mild (<0.5 G) rotating gravito-inertial vectors

4.1. Autonomic and pupil diameter effects on eye reflexes

Is pupil diameter simply a correlate of optokinetic gain due to central mechanisms, or does the amount of light falling on the retina (as determined by the iral aperture) directly affect the strength of the OKR? Our unilateral pilocarpine experiment suggests the former—that pupil diameter is simply a window on the central autonomic state of the animal. The observation that OKR gain increases during both wide and very narrow PD (with a trough around 1.5 mm) might be explained by independent sympathetic and parasympathetic circuitry. Both PD extremes could be considered an ‘arousal’ of the respective autonomic system, and could involve separate brainstem pathways.

A partial visual field is known to change the optokinetic response [38], but pupil diameter does not affect visual field size significantly. Pupil diameter has been shown to correlate with other behaviors, like the timing of bird song related to how much light falls on the retina [42]. Efferent projections to the gerbil retina from the lateral geniculate, pretectum, nuclei of the optic tract, and superior colliculus have been shown [24]. The possibility of a feedback loop between pupil diameter and orienting reflexes remains.

A circadian effect on vestibular reflexes would be an important parameter for adaptation studies. Gerbils are crepuscular (most active at dawn and dusk) [32,41], but our findings suggest that the state of the autonomic nervous system is quite different between dawn and dusk. A similar diurnal asymmetry is supported in recent work describing the cycles of Fos expression in the gerbil dorsal raphe nucleus [19], which receives retinal circadian inputs indirectly. Many studies have now demonstrated the effect of vestibular input on autonomic reflexes, e.g. Refs. [46,47]. It is unlikely that this interaction is unidirectional. Correlations between autonomic activity and vestibular sensitivity have also been made in humans [23].

4.2. Interaction of the optokinetic and vestibulo-ocular reflex

It seems clear that the vestibulo-ocular reflex cannot

really be considered an independent system [4,5,7]. But how and where does it interact with optokinetic reflexes? Accessory optic information reaches multiple levels of vestibular-related nuclei, i.e. the vestibulocerebellum through the pons and inferior olive, and direct projections to the vestibular and prepositus nuclei in the gerbil, rat, rabbit, cat [10,11,21,36] and monkey [27]. Our finding that an isoplanar optokinetic bias velocity linearly shifts the vestibular response velocity suggests a common final pathway to oculomotor neurons between vestibular and optokinetic systems. One likely pathway is floccular target neurons (FTNs) via activity in the dorsal cap, as unilateral olivary lesions created similar VOR velocity bias in rabbits [1].

Our data suggest a gated link between the vestibular and optokinetic systems in the gerbil. The rat has also been shown to cancel nystagmus well during optokinetic suppression [29]. The strong optokinetic suppression of the VOR, and conversely how vestibular input can re-engage a response to an ignored optokinetic stimulus, imply further interaction involving gated or inhibitory pathways. These findings likely also depend on or include autonomic or attentive factors. Optokinetic responses have been shown to depend on attention, or the 'look versus stare' paradigm in people [17,26]. However, there is also evidence that vestibular and optokinetic systems can act independently. In mice lacking the metabotropic glutamate receptor 1 gene, optokinetic—but not vestibular—adaptation was prevented [39].

Half-cycle direction-dependent horizontal VOR asymmetry in the dark was stronger in the same direction favored by optokinetic stimulation, i.e. during temporonasal motion. This observation was much more pronounced than the small optokinetic or saccadic asymmetries that might be based on eye muscle asymmetries in people [6,43]. Rather, this rotational vestibular asymmetry is again likely due to the organization of the OKR/VOR pathways on each side of the lateral-eyed brain. Vergence per say could be present in the gerbil, as shown in the rat during linear accelerations [16] and rabbit during target approach [48]. In rats, ~80° of the central visual field overlaps and is represented binocularly in the superior colliculus [9]. The drifting movements we observed in the dark, and during horizontal rotations in the dark, generated significant vergence (Fig. 7A, top trace), but these cannot be attributed to an otolith signal. Since the optic axes are directed laterally (~50°), and there is no system for foveal targeting, any relative slippage of eye position to the other in these cases is probably due to temporonasal asymmetries. Presumably this rotational 'dark vergence' needs no functional interpretation in the brain.

If the optokinetic and vestibulo-ocular systems are closely linked, one might expect that in the lateral-eyed rodent a temporonasal bias would also occur during vestibular-only responses. On the other hand, there does appear to be a greater degree of eye independence in such animals, for example, in often observed asynchronous pupil diameter changes. The emerging picture is one of a linked bilateral synchrony, with modular components.

4.3. The gerbil as an otolith model

Our oculomotor data in the gerbil is similar to that reported in other lateral-eyed species. Gravity, or the orientation of the otolith organs in gravity, is a key component of the VOR response in rat [3] and rabbit [2]. When the otolith organs are stimulated, the low frequency dynamics are extended. When the animal is turned upside down, large phase and gain differences result.

Linear centripetal forces generated by centrifuge rotation have significant static and dynamic effects on eye position and movement. For example, the angular VOR can be strongly suppressed during a centripetal stimulus, and longer-term exposure to increased inertial forces produces adaptation in the normal plane of the VOR response (data not shown). We also have preliminary data that dynamic otolith signals have a strong influence on the rotational VOR in the gerbil. Others have shown that the brain uses a gravito-inertial reference to modify the rotational VOR on a centrifuge [45], or to assist in the estimation of constant velocity during cross-coupling, probably through an interaction of the vertical canals with otolith signals [34]. In that monkey study (frontal-eyed), only pitch while rotating generated significant horizontal nystagmus, while both pitch or roll while rotating will do so in the gerbil. Our system is also capable of testing rotating gravito-inertial vectors (using counter-rotation similar to off-vertical axis rotation, or pseudo-OVAR), and angular and linear coriolis stimuli (pitch or roll while rotating and during linear forces). We have shown that the gerbil generates horizontal nystagmus during both pitch or roll while rotating stimuli, and also during mild rotating gravity vectors (cross-coupling and pseudo-OVAR). These subjects will be the focus of forthcoming papers, along with the effects of training and habituation during such stimuli.

The often overused term 'velocity storage' is a manifestation of the interconnections between spatial input systems. While the gerbil canal constant is short compared to primates; about 2 s [37], (and 2.3–4 s in the rat [8]) some evidence for velocity storage in rodents does exist. The rat horizontal SPEV time constant to head step velocity was measured to be approximately two times the canal constant [29]. The time constant of the response decrement following the roll cross-coupling stimulus in Fig. 8A, for example, was also greater than the canal constant. From an optokinetic perspective, the mean time constant for optokinetic after nystagmus in the rat is about 8 s [15], and the velocity sensitivity during constant velocity optokinetic stimulation extends far above that of sinusoidal stimuli in rodents. Therefore at least a rudimentary motion memory happens in the interaction of vestibular and optokinetic systems in the rodent. The attributes and anatomy of this interaction remain to be fully described.

Video-oculography provides accurate before and after comparisons and additional autonomic data during behaving experiments. Although the limitations of our device in terms of sampling frequency and vertical and torsional eye motion require careful consideration, improvements are certainly possible, and the relative ease in which high-quality, non-invasive binocular data can be acquired makes this an important new tool for eye movement studies in small animals.

Acknowledgements

Bill Crosier, EE, coordinated the centrifuge design and development, and was invaluable in its success. Robert Orton, ME, assisted with mechanical design, and Randy Riggs, implemented software solutions in LabView. I thank John Dawson for his excellent technical assistance. Mike Shinder's thesis-related experiments also had a significant role in shaping these methods. Chris Livingston reviewed early drafts and provided valuable suggestions. Supported by NIH RO1 DC-04170.

References

[1] N. Barmack, J. Simpson, Effects of microlesions of dorsal cap of inferior olive of rabbits on optokinetic and vestibuloocular reflexes, J. Neurophysiol. 43 (1980) 182–206.
[2] N.H. Barmack, The influence of gravity on horizontal and vertical vestibulo-ocular and optokinetic responses in the rabbit, Brain Res. 424 (1987) 89–98.
[3] S.C. Brettler, S.A. Rude, K.J. Quinn, J.E. Killian, E.C. Schweitzer, J.F. Baker, The effect of gravity on the horizontal and vertical vestibulo-ocular reflex in the rat, Exp. Brain Res. 132 (2000) 434–444.
[4] H. Collewijn, The vestibulo-ocular reflex: an outdated concept, Prog. Brain Res 80 (1989) 197–209, Discussion on pp. 171–172.
[5] H. Collewijn, The vestibulo-ocular reflex: is it an independent subsystem?, Rev. Neurol. (Paris) 145 (1989) 502–512.
[6] H. Collewijn, C. Erkelens, R. Steinman, Binocular co-ordination of human horizontal saccadic eye movements, J. Physiol. 404 (1988) 157–182.
[7] A.C. Cova, H.L. Galiana, A bilateral model integrating vergence and the vestibulo-ocular reflex, Exp. Brain Res. 107 (1996) 435–452.
[8] I.S. Curthoys, The response of primary horizontal semicircular canal neurons in the rat and guinea pig to angular acceleration, Exp. Brain Res. 47 (1982) 286–294.
[9] Y. Diao, Y. Wang, Y. Xiao, M. Bu, Binocular responses in the superior colliculus of the albino rat, Sci. Sin. B 27 (1984) 1245–1254.
[10] R.A. Giolli, R.H. Blanks, Y. Torigoe, Pretectal and brain stem projections of the medial terminal nucleus of the accessory optic system of the rabbit and rat as studied by anterograde and retrograde neuronal tracing methods, J. Comp. Neurol. 227 (1984) 228–251.
[11] R.A. Giolli, R.H. Blanks, Y. Torigoe, D.D. Williams, Projections of medial terminal accessory optic nucleus, ventral tegmental nuclei, and substantia nigra of rabbit and rat as studied by retrograde axonal transport of horseradish peroxidase, J. Comp. Neurol. 232 (1985) 99–116.
[12] V. Govardovskii, P. Rohlich, A. Szel, T. Khokhlova, Cones in the retina of the Mongolian gerbil, *Meriones unguiculatus*: an immunocytochemical and electrophysiological study, Vision Res. 32 (1992) 19–27.
[13] W. Graf, Spatial coordination of compensatory eye movements in vertebrates: form and function, Acta Biol. Hung. 39 (1988) 279–290.
[14] R. Harvey, C. De'Sperati, P. Strata, The early phase of horizontal optokinetic responses in the pigmented rat and the effects of lesions of the visual cortex, Vision Res. 37 (1997) 1615–1625.
[15] B. Hess, W. Precht, A. Reber, L. Cazin, Horizontal optokinetic ocular nystagmus in the pigmented rat, Neuroscience 15 (1985) 97–107.
[16] B. Hess, N. Dieringer, Spatial organization of linear vestibuloocular reflexes of the rat: responses during horizontal and vertical linear acceleration, J. Neurophysiol. 66 (1991) 1805–1818.
[17] S. Holm-Jensen, The significance of attention and duration of the stimulation in optokinetic nystagmus, Acta Otolaryngol. 98 (1984) 21–29.
[18] G. Jacobs, J.n. Deegan, Sensitivity to ultraviolet light in the gerbil (*Meriones unguiculatus*): characteristics and mechanisms, Vision Res. 34 (1994) 1433–1441.
[19] S. Janusonis, K. Fite, Diurnal variation of c-Fos expression in subdivisions of the dorsal raphe nucleus of the Mongolian gerbil (*Meriones unguiculatus*), J. Comp. Neurol. 440 (2001) 31–42.
[20] C. Jeon, E. Strettoi, R. Masland, The major cell populations of the mouse retina, J. Neurosci. 18 (1998) 8936–8946.
[21] G.D. Kaufman, M.J. Mustari, R.R. Miselis, A.A. Perachio, Transneuronal pathways to the vestibulocerebellum, J. Comp. Neurol. 370 (1996) 501–523.
[22] G.D. Kaufman, M.E. Shinder, A.A. Perachio, Spatiotemporal properties of perihypoglossal neurons in the gerbil, J. Neurophys. (1999) in press.
[23] L. Kornilova, A. Solov'eva, V. Oknin, N. Arlashchenko, Effect of the character of autonomic response and the emotional and personality features of a human being on reactions of the vestibular system, Hum. Physiol. 25 (1999) 549–554.
[24] J. Larsen, M. Moller, Evidence for efferent projections from the brain to the retina of the Mongolian gerbil (*Meriones unguiculatus*). A horseradish peroxidase tracing study, Acta Ophthalmol. Suppl. 173 (1985) 11–14.
[25] K. Long, S. Fisher, The distributions of photoreceptors and ganglion cells in the California ground squirrel *Spermophilus beecheyi*, J. Comp. Neurol. 221 (1983) 329–340.
[26] D.R. Mestre, G.S. Masson, Ocular responses to motion parallax stimuli: the role of perceptual and attentional factors, Vision Res. 37 (1997) 1627–1641.
[27] M.J. Mustari, A.F. Fuchs, C.R. Kaneko, F.R. Robinson, Anatomical connections of the primate pretectal nucleus of the optic tract, J. Comp. Neurol. 349 (1994) 111–128.
[28] S. Nagao, A non-invasive method for real-time eye position recording with an infrared TV-camera, Neurosci. Res. 8 (1990) 210–213.
[29] M. Niklasson, R. Tham, L. Odkvist, Vestibular disturbances after neck muscle sectioning in rat, Acta Otolaryngol. Suppl. 449 (1988) 85–88.
[30] A.A. Perachio, M.J. Correia, Responses of semicircular canal and otolith afferents to small angle static head tilts in the gerbil, Brain Res. 280 (1983) 287–298.
[31] A. Pereira, E. Volchan, C. Vargas, L. Penetra, C. Rocha-Miranda, Cortical and subcortical influences on the nucleus of the optic tract of the opossum, Neuroscience 95 (2000) 953–963.
[32] A.T. Pietrewicz, M.P. Hoff, S.A. Higgins, Activity rhythms in the Mongolian gerbil under natural light conditions, Physiol. Behav. 29 (1982) 377–380.
[33] K.J. Quinn, S.A. Rude, S.C. Brettler, J.F. Baker, Chronic recording of the vestibulo-ocular reflex in the restrained rat using a permanently implanted scleral search coil, J. Neurosci. Methods 80 (1998) 201–208.
[34] T. Raphan, M. Dai, J. Maruta, W. Waespe, V. Henn, J.I. Suzuki, B.

Cohen, Canal and otolith afferent activity underlying eye velocity responses to pitching while rotating, Ann. NY Acad. Sci. 871 (1999) 181–194.
[35] T. Raphan, V. Matsuo, B. Cohen, Velocity storage in the vestibulo-ocular reflex arc (VOR), Exp. Brain Res. 35 (1979) 229–248.
[36] M. Schmidt, D. Schiff, M. Bentivoglio, Independent efferent populations in the nucleus of the optic tract: an anatomical and physiological study in rat and cat, J. Comp. Neurol. 360 (1995) 271–285.
[37] L. Schneider, D. Anderson, Transfer characteristics of first and second order lateral canal vestibular neurons in gerbil, Brain Res. 112 (1976) 61–76.
[38] C. Schor, V. Narayan, The influence of field size upon the spatial frequency response of optokinetic nystagmus, Vision Res. 21 (1981) 985–994.
[39] F. Shutoh, A. Katoh, H. Kitazawa, A. Aiba, S. Itohara, S. Nagao, Loss of adaptability of horizontal optokinetic response eye movements in mGluR1 knockout mice, Neurosci. Res. 42 (2002) 141–145.
[40] J.S. Stahl, A.M. van Alphen, C.I. De Zeeuw, A comparison of video and magnetic search coil recordings of mouse eye movements, J. Neurosci. Methods 99 (2000) 101–110.
[41] V. Susic, G. Masirevic, Sleep patterns in the Mongolian gerbil *Meriones unguiculatus*, Physiol. Behav. 37 (1986) 257–261.
[42] R. Thomas, T. Szekely, I. Cuthill, D. Harper, S. Newson, T. Frayling, P. Wallis, Eye size in birds and the timing of song at dawn, Proc. R. Soc. Lond. B 269 (2002) 831–837.
[43] A. Van den Berg, H. Collewijn, Directional asymmetries of human optokinetic nystagmus, Exp. Brain Res. 70 (1988) 597–604.
[44] J. Van der Geest, M. Frens, Recording eye movements with video-oculography and scleral search coils: a direct comparison of two methods, J. Neurosci. Methods 114 (2002) 185–195.
[45] S. Wearne, T. Raphan, B. Cohen, Effects of tilt of the gravito-inertial acceleration vector on the angular vestibuloocular reflex during centrifugation, J. Neurophysiol. 81 (1999) 2175–2190.
[46] B.J. Yates, Vestibular influences on the sympathetic nervous system, Brain Res. Rev. 17 (1992) 51–59.
[47] B.J. Yates, A.D. Miller, Physiological evidence that the vestibular system participates in autonomic and respiratory control, J. Vestib. Res. 8 (1998) 17–25.
[48] I. Zuidam, H. Collewijn, Vergence eye movements of the rabbit in visuomotor behavior, Vision Res. 19 (1979) 185–194.